RESEARCH ARTICLE | FEBRUARY 17 2016

New experimental capability to investigate the hypervelocity micrometeoroid bombardment of cryogenic surfaces

Andrew Oakleigh Nelson; Richard Dee; Murthy S. Gudipati; Mihály Horányi; David James; Sascha Kempf; Tobin Munsat; Zoltán Sternovsky; Zach Ulibarri

Rev. Sci. Instrum. 87, 024502 (2016)
https://doi.org/10.1063/1.4941960

New experimental capability to investigate the hypervelocity micrometeoroid bombardment of cryogenic surfaces

Andrew Oakleigh Nelson,[1,2,a)] Richard Dee,[1] Murthy S. Gudipati,[3] Mihály Horányi,[1,4] David James,[1,4] Sascha Kempf,[1,2,4] Tobin Munsat,[1,2] Zoltán Sternovsky,[1,4,5] and Zach Ulibarri[1,2]

[1]*Institute for Modeling Plasma, Atmospheres and Cosmic Dust (IMPACT), University of Colorado, Boulder, Colorado 80309, USA*
[2]*Department of Physics, University of Colorado, Boulder, Colorado 80309, USA*
[3]*Science Division, Jet Propulsion Laboratory, California Institute of Technology, 4800 Oak Grove Drive, Pasadena, California 91109, USA*
[4]*Laboratory for Atmospheric and Space Physics, 1234 Innovation Drive, Boulder, Colorado 80303, USA*
[5]*Aerospace Engineering Sciences, University of Colorado, Boulder, Colorado 80309, USA*

(Received 30 November 2015; accepted 1 February 2016; published online 17 February 2016)

Ice is prevalent throughout the solar system and beyond. Though the evolution of many of these icy surfaces is highly dependent on associated micrometeoroid impact phenomena, experimental investigation of these impacts has been extremely limited, especially at the impactor speeds encountered in space. The dust accelerator facility at the Institute for Modeling Plasmas, Atmospheres, and Cosmic Dust (IMPACT) of NASA's Solar System Exploration Research Virtual Institute has developed a novel cryogenic system that will facilitate future study of hypervelocity impacts into ice and icy regolith. The target consists of a copper block, cooled by liquid nitrogen, upon which layers of vapor-deposited ice, pre-frozen ice, or icy regolith can be built in a controlled and quantifiable environment. This ice can be grown from a variety of materials, including H_2O, CH_3OH, NH_3, and slurries containing nanophase iron. Ice temperatures can be varied between 96 K and 150 K and ice thickness greater than 150 nm can be accurately measured. Importantly, the composition of ion plumes created during micrometeoroid impacts onto these icy layers can be measured even in trace amounts by *in situ* time-of-flight mass spectroscopy. In this paper, we present the fundamental design components of the cryogenic target chamber at IMPACT and proof-of-concept results from target development and from first impacts into thick layers of water ice. [http://dx.doi.org/10.1063/1.4941960]

I. INTRODUCTION

In recent decades, a series of discoveries have shown that many worlds previously thought to be entirely dehydrated actually contain a significant amount of water in the form of ice. For example, water ice deposited by impacts of comets, meteorites, and solar wind protons has been found in various forms in the Moon's interior, in the lunar surface regolith and in cold traps at the lunar poles.[1] Additional complex ice environments are prevalent throughout the solar system, especially beyond the frost line. Most notably, ice is found on the surface of Mars, on the Jovian satellites Europa, Ganymede, and Callisto, in Saturnian satellites such as Enceladus and Titan, on Neptune's Triton, in comets from the Oort cloud, and, most recently, on Pluto and Charon.[2–4]

The frequent bombardment of ice and icy surfaces by micrometeoroids with diameters of ~1 μm plays a major role in the evolution of satellite surfaces and planetary rings in the outer solar system.[2] Select experiments conducted by Burchell *et al.*,[5,6] Eichhorn and Grün,[7] Koschny and Grün,[8] and Timmermann and Grün[9] have established initial investigations into the cratering, erosion, and redistribution phenomena associated with hypervelocity micrometeoroid impacts into water ice. Burchell *et al.* used a light gas gun to examine the impact light flash and ionization from hypervelocity impacts into ice[5] in addition to the cratering depth and diameter of impacts into water ice.[6] These studies used larger particles with diameters of ~1 mm and velocities near ~5 km/s. With an electrothermal accelerator, Eichhorn and Grün extended the knowledge of crater formation on icy surfaces by measuring the vapor release associated with hypervelocity impacts into water ice by micrometeoroids with diameters less than 10 μm and velocities in the range of 1 to 50 km/s.[7] Most recently, Koschny and Grün conducted detailed cratering studies of impacts into ice-silicate mixtures by micrometeoroids traveling with velocities between 1 km/s and 12 km/s, further expanding the understanding of cratering phenomena on icy surfaces.[8] Finally, Timmermann and Grün performed preliminary measurements of ion mass spectra from hypervelocity (3–60 km/s) impacts into water ice. The above investigations laid essential foundations regarding the characterization of ice impacts, but detailed investigation of the quantity, velocity, and angular distribution of ions and ejecta has yet to be conducted.

Furthermore, the scientific understanding needed to link impact-produced ions to the icy surfaces from which they were produced is not fully developed. Specific data sets of

a)andrew.nelson-1@colorado.edu

ice particles from Saturn's E-ring[10] and from Enceladus' ice volcanoes[11] have demonstrated that dust analysis measurements of both ice and non-ice particles are among the most sensitive tools for determining the compositions of icy surfaces.[12] Yet dust facilities[13,14] capable of the hypervelocity acceleration necessary for these investigations have focused on research using standard (non-ice) dust and target compositions while impacts into icy surfaces remain largely unexplored. The cryogenic target at the Institute for Modeling Plasmas, Atmospheres, and Cosmic Dust (IMPACT) is uniquely suited to help acquire a more thorough understanding of the composition of ion plumes from icy impacts. This work has many applications including the calibration of *in situ* science instruments such as the successful Cosmic Dust Analyzer on Cassini[15] and the upcoming SUrface Dust Analyser (SUDA), selected to fly on the Europa mission.[16]

Recent work has also shown that the micrometeoroid bombardment of icy surfaces can produce various complex organic materials.[17,18] These organics may comprise a core of biologically significant molecules that migrate between planetary bodies, including an early Earth, in impact plumes.[19,20] The survival of surface organics in hypervelocity impact plumes has been modeled for impactors with a diameter of several km[21] and directly studied for impactors of ~1 mm[20] diameter, but not for micrometeoroids. The synthesis and transport of these molecules to Earth could have enormous significance in the search for the origins of life.

Even though they are clearly present throughout the solar system and beyond, the detailed formation mechanisms of these complex organics are not yet well understood. While several groups have exposed potential pathways toward biologically relevant molecules in the laboratory by bombarding ice with large dust impactors, protons, electrons, and UV irradiation,[17,22–24] only recently has direct mass analysis of irradiation products been conducted.[25] In that research, Henderson and Gudipati demonstrated that complex organics such as formamide and acetamide are produced under electron and UV bombardment of astrophysical ice analogs.[25] Similarities exist between laser ionization and impactionization,[28] but these complex organic reactions have yet to be studied directly under hypervelocity micrometeoroid bombardment.

The new cryogenic target recently developed at the dust accelerator at the IMPACT facility at the University of Colorado, Boulder is capable of directly addressing several open questions related to the study of impacts into ice and icy regolith. Among these research areas are the production of relevant scaling laws for impact-produced ejecta over a wide range of projectile parameters, the mapping of ion plume composition for various target and projectile materials, and the investigation of complex organic reactions characteristic of impacts into icy surfaces containing non-icy particles including nanophase iron and silicate grains.

To further this research, frozen targets can be prepared under a wide range of conditions designed to replicate simulated volatile-rich icy asteroid surfaces. Possible targets include layers of vapor-deposited H_2O, CH_3OH, and NH_3 ices, pre-frozen slurries of various compounds (including nanophase iron), and all combinations thereof. Additionally, target temperature is controllable and can be varied between 96 K and 150 K. These targets can be directly exposed to hypervelocity impacts from a well-controlled dust source, where projectile composition, velocity, and size can be individually selected. Ejecta from these impacts, such as water clusters or complex organic chains and fragments, can be identified even in trace amounts by *in situ* time-of-flight (TOF) mass spectroscopy. Furthermore, as a result of the flexible design of this chamber, future experimental improvements will allow measurements to be simultaneously collected from various diagnostic instruments, such as an infrared spectrometer, in order to cross-calibrate detectors.

In this article, we outline the technical details of this new cryogenic facility, comment on the experimental capabilities of this system, and present proof-of-concept mass spectra for micrometeoroid impacts into water ice with thicknesses up to 20 μm.

II. EXPERIMENTAL SETUP

A schematic overview of the new experimental assembly capable of hypervelocity impact studies on cryogenic surfaces is shown in Fig. 1. Fig. 2 shows a photo of the ice chamber. During experimental operation, dust particles of up to 2 μm in diameter are individually selected from the 3 MV hypervelocity IMPACT Dust Accelerator[13] to fit within specified velocity ranges between 1 and 100 km/s. These iron particles enter into the chamber from the right and collide with an icy surface sitting at high (up to ±3.5 kV) voltage. Ions created in this impact are accelerated through a grounded grid towards a time-of-flight mass spectrometer.

Most of the critical new components in this system are associated with the ice growth process. Pure ice surfaces are grown through vapor deposition, which is carefully controlled by manipulating the vapor pressure in the chamber while maintaining a set target temperature with an integrated liquid nitrogen (LN_2) flow and heater loop. This process is monitored

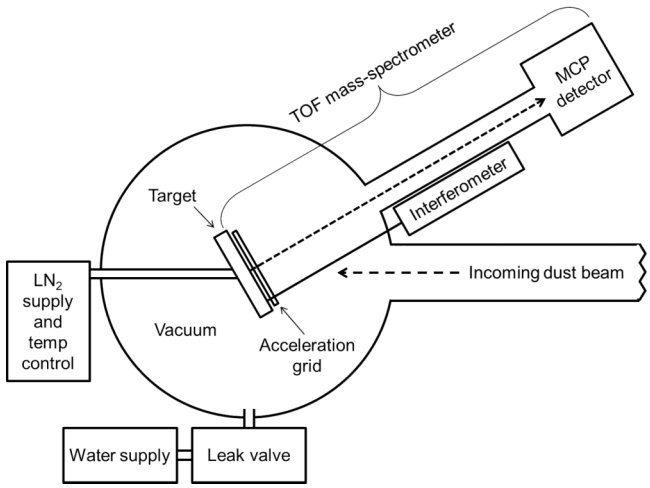

FIG. 1. Essential components of the cryogenic target. Charged ejecta, which are created upon the collision of dust particles with the icy target, are accelerated to an *in situ* time-of-flight (TOF) mass spectrometer. Ice thickness is carefully controlled using a leak valve and monitored using fringe-counting interferometry.

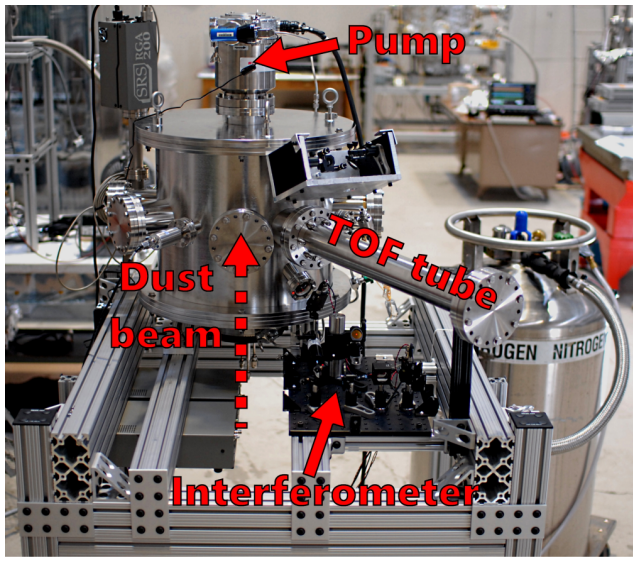

FIG. 2. A photo of the IMPACT ice chamber. In this photo, the chamber is removed from the beam line.

using an *in situ* interferometer to provide measurements of ice growth rate and ice thickness. The copper target plate and the ice target are electrically and partially thermally isolated from the rest of the assembly by a thin Kapton sheet. The essential subcomponents of the chamber are described in greater detail below.

A. The cryogenic system

Ice is grown by vapor deposition onto a gold-coated sapphire substrate that is kept cold by an integrated cryogenic system, which consists of a copper target plate, a copper block, and LN_2 feed tubes, as shown in Fig. 3. The copper target plate and sapphire substrate are kept cold by a copper block, which in turn is cooled via direct contact with flowing LN_2. For the current setup shown in Fig. 3, where the LN_2 feed enters from below, a continuous flow of LN_2 is required to avoid build up of nitrogen gas in the Cu cooling block, which could compromise effective temperature control. Liquid nitrogen is pumped directly through the Cu cooling block whenever the block's temperature needs to be lowered. Under extended uninterrupted flow, the cooling block and ice surface can reach temperatures as low as 76.4 K (the boiling point of LN_2 at an altitude of 1655 m) and 96.5 K, respectively. The ice surface can reach even lower temperatures if the heater is removed, which improves thermal contact between the copper target plate and the copper block. Ice growth has been observed at all accessible temperatures below 150 K.

The chamber is constructed in such a way that the target can also be inserted from the top and sides of the chamber. For the case in which the copper block is below the LN_2 feed, liquid can remain resident in the block and feed pipes. When the target is inserted sideways, continuous LN_2 flow is needed. These orientations are easily interchangeable and can be manipulated as an additional degree of freedom to ease the construction of complex target surfaces.

In ordinary operation, Si diode thermometers are mounted on the cooling block and the copper target plate. In combination with a thin-film Kapton-insulated heater, these thermometers allow for precise control of the target plate temperature, reducing variation to tenths of a Kelvin. In the current design, the target-side thermometer shown in Fig. 3 is connected directly to the copper target plate, which is slightly thermally isolated from the ice surface by the sapphire substrate. The cooling block thermometer is not shown. Further improvements to this design are currently being implemented and will allow for direct control of the substrate surface temperature through a controlled feedback loop.

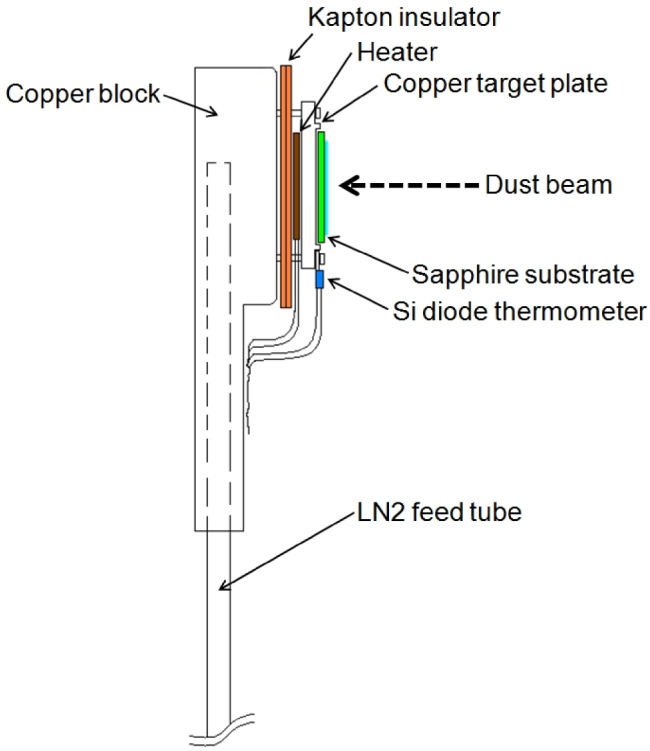

FIG. 3. Side view of the ice target. The copper target plate is attached with four PEEK screws through the Kapton insulation. A sapphire substrate is attached to the target plate with Apiezon N Grease.

B. Ice targets

Various types of ice targets can be formed using interchangeable copper target backing plates. In general, the target quality/type/source is determined by the user, but for these initial tests laboratory-prepared distilled water was used. Future targets will include additional compounds such as methanol and ammonia ice samples. Ice can be produced in two ways: pre-freezing from liquid in a shallow recess or *in situ* ice growth from vapor deposition. For the latter case, a smooth, optical-quality sapphire plate is used as a substrate for the ice growth. The sapphire is coated with a bi-layer of titanium and gold to provide both an electrically conducting plane and a reflective surface for laser interferometer measurements. This substrate is held in a shallow recess in the copper target plate with a thin layer of Apiezon N Grease to ensure adhesion and thermal contact. N grease exhibits a vapor pressure of less than 8×10^{-10} mbar at cryogenic temperatures and is therefore not a contaminant concern. As shown in Fig. 3, the target plate is separated from the copper cooling plate by both the

heater and by a wide but thin Kapton insulator and is bolted onto the cooling block with four insulating PEEK screws. The ice target is therefore electrically and partially thermally isolated from the rest of the system and can be routinely raised to accelerating voltages as high as ±3.5 kV for mass spectroscopy purposes. The thickness of the Kapton sheet (127 μm) was chosen to provide enough thermal isolation to allow for direct temperature control of the copper target plate against a liquid nitrogen background and enough electrical insulation to serve as a high voltage standoff between the grounded copper cooling block and the copper target plate.

A photo of the ice target is provided in Fig. 4, where two additional features of the setup are visible. First, Fig. 4 shows that the copper cooling block is connected to a thick steel beam with a thermally isolating Delrin bolt. While this connection is necessary to increase structural support and stabilize the ice target against vibrations, it also provides alignment control as the Delrin bolt can be adjusted to change the angle of the target surface from vertical. Additionally, Fig. 4 shows an optional vapor-delivery tube that was originally included in order to provide more control over the vapor-deposited ice growth. Using techniques for producing vapor-grown ice layers inspired by Henderson and Gudipati,[25] this delivery tube proved unnecessary and was removed. Ice is now deposited in the following manner. After the sapphire substrate has been cooled to a pre-determined temperature below 160 K, water vapor is allowed to leak into the chamber at a steady rate using the leak valve shown in Fig. 1 until the chamber pressure rises from a base pressure of approximately 7×10^{-8} mbar to a set value in the range of (5–150) $\times 10^{-6}$ mbar. When individual water molecules come in contact with the substrate, they freeze and adhere to the surface. The ice growth proceeds at a steady rate that is directly measured with an *in situ* interferometer. Exact growth rates are a function of the compound and the chamber pressure but are on the order of 1 μm of additional ice growth every ~750 s.

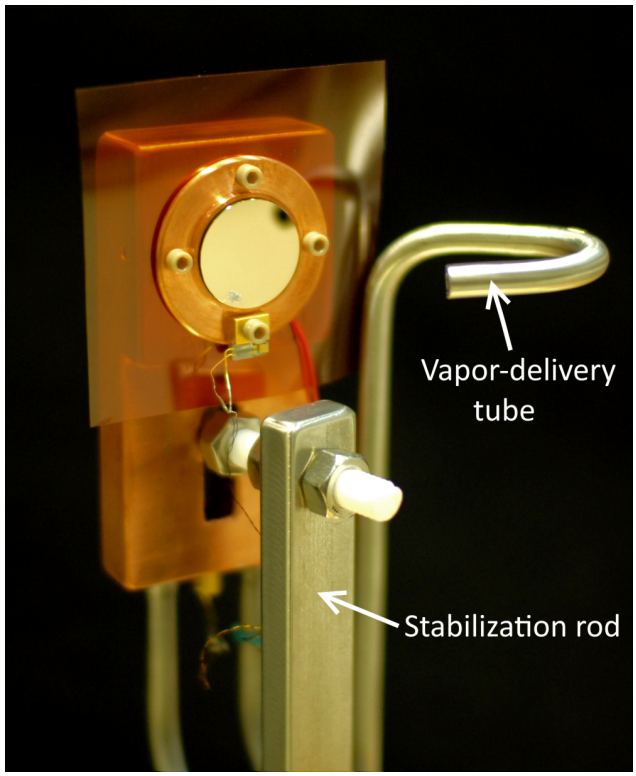

FIG. 4. A photo of the front of the ice target, including an optional vapor-administration tube. The copper block is stabilized by a thermally insulating connection with a thick steel beam.

Once the desired ice thickness has been reached, the water supply is closed off from the chamber, which is then allowed to pump down to its original base pressure. Ice grown in this way remains on the substrate surface for arbitrarily long periods of time without noticeable thickness reduction due to sublimation, provided that the substrate remains at low temperatures. If the target is allowed to warm to room temperature, ice frozen on the LN_2 supply tubes, the copper blocks, and the substrate begins to sublimate, causing significant pressure jumps in the chamber. Sublimation fringe patterns caused by a decrease in ice film thickness have been observed at temperatures near 180 K and consistently match the respective ice growth patterns.

Capabilities that will enable investigations of ejecta from dust impacts into targets that are not vapor-grown are currently being developed. Importantly, the cryogenic chamber at IMPACT will be able to accommodate pre-frozen liquid targets and slurry targets including silicates or other regolith stimulants without extensive design modification. This is made possible by the interchangeable copper backing plates used to hold each target sample and the easily adjusted rotating flange upon which the target apparatus rests.

Initial test-targets containing Olivine mixtures have been prepared to refine and test the feasibility of the following method for producing slurry targets. Olivine ($(Mg^{+2}, Fe^{+2})SiO_4$) is a silicate rich in magnesium and iron that occurs naturally in igneous rock; replicated samples of this material were obtained from Physics Department at the University of Central Florida. Dry Olivine samples can be wet using water, methanol, and ammonia mixtures to create a variety of target mixtures, slurries, and pastes. These targets are then frozen with liquid nitrogen while submersed in an N_2 background gas at atmospheric pressure. Once the targets are frozen, they are inserted into the vacuum chamber, which has been pre-filled with N_2 gas to reduce condensation effects. After the chamber has reached vacuum pressures, additional layers of vapor-deposited compounds may be deposited onto the surface of the target in controlled amounts using pre-calibrated growth rates. The ability to manufacture complex targets containing nanophase iron is essential to replicating volatile-rich icy asteroid surfaces, extending chemical analysis work[25] conducted on vapor-deposited targets.

C. Interferometry

Throughout the growth process, light from a 0.8 mW, polarized HeNe laser is incident on both the ice and substrate surfaces, producing characteristic Fabry-Perot interference patterns. An overview of the interferometer beam path is shown in Fig. 5. After passing through an adjustable neutral density filter that brings the signal level to within the dynamic range of the two Si biased detectors [Thorlabs DET100A], the beam passes through a 70% transmittance beam-splitter. At

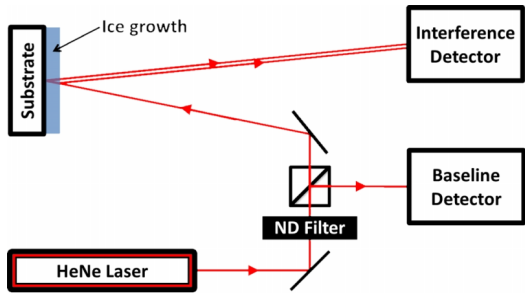

FIG. 5. The interferometer beam path. Interference from the two beam paths leaving the substrate and ice surfaces produces measurable fringes that correspond to ice growth.

this point, 30% of the beam is diverted to the first detector in order to measure base fluctuations in laser power. Most of the beam passes into the vacuum chamber where it reflects off of both the substrate and ice surfaces. The thin ice film and the gold-coated sapphire substrate form a Fabry-Perot interferometer, such that measurable fringe patterns corresponding to ice growth are observed at the second detector.

An example fringe pattern is shown in Fig. 6, where each fringe corresponds to 0.27 μm of additional ice growth according to

$$2d\cos(\theta) = m\frac{\lambda}{n},$$

where d is the thickness of the ice, $\lambda = 632.8$ nm is the wavelength of the HeNe laser, $n = 1.31$ is the index of refraction of ice, $\theta = 25°$ is the angular offset of the interferometer, and m is the number of fringes. The interferometer signal tends to decay with time either as a result of increased attenuation within thicker ice or of scattering from uneven ice surfaces. The exact physics of this phenomenon will be investigated at a later time. However, the ice growth rate does not vary significantly at any point, allowing for the precise calculation of ice thickness even for very thick ice layers that no longer produce visible fringes.

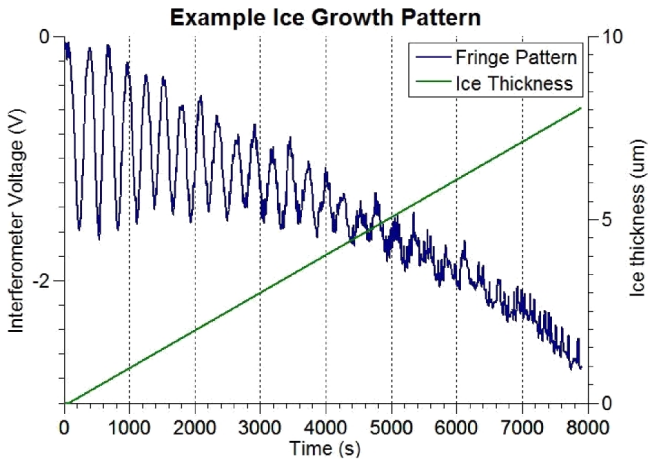

FIG. 6. A typical ice growth interference pattern. In this sample the total ice thickness reached 8.02 μm at a chamber pressure of $P = 6.7\times10^{-6}$ mbar before ice growth was stopped. Total laser power begins to diminish significantly after about 4 μm of ice growth.

D. TOF mass spectrometer

During experimental operation, the chamber is held at a base pressure of $\sim7\times10^{-8}$ mbar with a turbomolecular pump. The copper target plate and the ice/slurry target are held at a high voltage up to ±3.5 kV. Particles accelerated from the 3 MV hypervelocity dust accelerator are centered onto the target. Upon collision, these particles produce clouds of ions and ejecta. The ions are accelerated towards a dual microchannel plate (MCP) detector via a grounded grid located approximately 0.5 cm from the high voltage target surface. Since current investigations are limited to studies of the relative strengths of mass lines only, this distance is not critical. In order to increase mass resolution, the MCP is housed at the end of a 1 m long evacuated tube, which extrudes from the main chamber in the plane of the incoming dust beam at an angle of 30° from the dust beam line. This arrangement requires precise control over the angle of the target and acceleration grid. While the acceleration grid is permanently attached and aligned to the TOF tube, the entire target apparatus must be removed for periodic modification and maintenance. In order to ensure proper alignment normal to the TOF tube, the target is mounted on a special rotatable vacuum flange with a 180° rotation range. Target alignment was found to be less critical than was originally expected with spectra signals on the MCP detector being measurable for target angles up to 5° off of normal in either direction, though further analysis of precise angular dependence is needed. Time-of-flight mass spectra are recorded separately for each impact and are saved for off-line data analysis.

III. RESULTS

A. Ice growth

As mentioned in Section II B, each additional interferometer fringe represents a 0.27 μm of ice growth. However, both the vapor pressure and target temperature within the chamber during the ice growth process have specific and substantial effects on the ice growth rate and on the quality of the resulting ice. As shown in Fig. 6, ice growth at a chamber pressure of $P = 6.7\times10^{-6}$ mbar and a target temperature of 150 K occurs at about 1 μm per ~1000 s. Furthermore, the ice crystals become visible and appear foggy after about 7.5 μm of ice has been deposited, at which point the interferometer interference signals are no longer distinguishable above the noise floor. In contrast, a chamber pressure of $P = 1.3\times10^{-5}$ mbar and a target temperature around 96 K result in a faster growth rate: an additional micron of ice growth every ~650 s. Ice grown under these conditions remains clear throughout the growth process, though a noticeable loss in interferometer power begins at thicknesses above 13 μm, as seen in Fig. 7.

The *in situ* interferometer allows for precise monitoring of ice growth under a wide range of parameters and with a variety of compounds. In combination with flexible temperature command and variable control of the water-vapor pressure within the chamber, this system opens up opportunities to grow and study ice layers of various thicknesses and crystalline structures. Higher water pressures correspond monotonically to faster ice growth, which has unexplored implications on

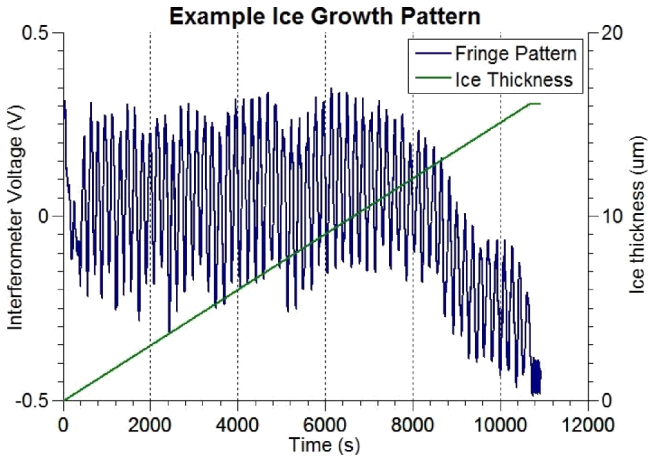

FIG. 7. An additional ice growth interference pattern. In this sample the total ice thickness reached 16.10 μm at a chamber pressure of $P = 1.3 \times 10^{-5}$ mbar before ice growth was stopped at 10 700 s. Total laser power begins to diminishes significantly after about 13 μm of ice growth.

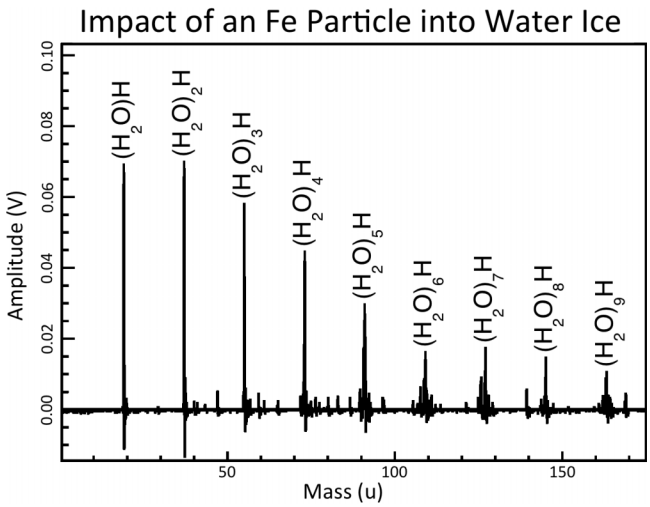

FIG. 8. An example mass spectrum of ejecta from dust impact into semi-infinite water ice. Characteristic clusters of water molecules with hydrogen are immediately evident, as is the absence of common contaminants such as carbon and atomic oxygen from the breakup of organics. This spectrum was measured after the impact of an iron particle with a radius of 83 nm that was traveling at 13.3 km/s.

ice crystal structure. Furthermore, ice grown at different substrate temperatures exhibits different physical properties,[3,26,27] which can be exploited to broaden understanding of dust-ice interactions in outer space. We note here that 96 K deposition results in amorphous ice with higher porosity, whereas 150 K deposition leads to the formation of hexagonal crystalline ice.[3,27] At 150 K, slow sublimation of ice is in competition with ice formation, resulting in the fogging of the ice surface mentioned above.

B. Ion plume composition

Initial measurements of the mass spectra of ions created from dust impacts have yielded promising results. Mass spectra have been recorded for a variety of particle sizes (10–5000 nm diameter) and velocities (1–100 km/s) and under various target voltages (±(1.5–3.5) kV) and angles (±5° from TOF axis). Under normal operation, spectra are recorded several times per minute. Preliminary analysis of spectra recorded with a blank substrate and for water ice targets of various thicknesses has shown that spectra can be obtained for all parameter combinations, though further optimization of target conditions is necessary in order to reduce noise levels and optimize signal strength.

A typical mass spectrum of the ion plume created by a ~2 μm diameter Fe particle impacting thick water ice is shown in Fig. 8. This spectrum was obtained with an ice thickness of 15.6 μm, which is several times greater than the expected crater depth in water ice. The impactor was a 166 nm diameter (1.9×10^{-17} kg) iron particle traveling at 13.3 km/s. It is immediately evident from these spectra that water clusters, which are characteristic of dust impacts into water ice, are produced during collision events at IMPACT. These clusters have been observed as groups of water molecules bonded with a singly ionized hydrogen, sodium, or potassium atom. In the spectrum shown in Fig. 8, only clusters with hydrogen are shown. Similar spectral compositions have been observed in data taken from water vapor and ice particle plumes on Enceladus.[11]

Importantly, initial spectra results display no evidence of organic contamination. Past work conducted by Timmermann and Grün has shown that mass spectra are extremely sensitive to trace contaminants on the target and impactor surfaces and that these contaminants are extremely difficult to remove.[9] However, the spectra taken for impacts into thick-film ice at IMPACT contain no evidence of lithium, carbon, carbon hydrates, silicon pump oil, or atomic oxygen from the breakup of organics. The absence of these contaminants demonstrates the cleanliness of this setup, which is essential for the future investigation of organic spectra. Sodium and potassium concentrations are, in general, present in these spectra and are the result of contaminants on the surface of impacting dust projectiles that will be extremely difficult to remove.

In addition to encouraging results relating to the cleanliness of the spectra, initial results also demonstrated several issues of concern. Unexplained features including low-level spectral lines corresponding to non-integer masses and excessive ringing in the TOF signal currently compromise detailed spectra analysis. Techniques to improve the purity of vapor-grown targets and other efforts to reduce the prevalence of these "ghost" lines are currently under investigation.

IV. CURRENT AND FUTURE WORK

Current work on the cryogenic target at IMPACT consists primarily of further preliminary testing of chamber capabilities and more detailed analysis of recovered mass spectra. Specifically, recent experimental trials have included analysis of dust impacts into blank targets, vapor-grown targets of higher-purity water and methanol, slurry targets consisting of pre-frozen Olivine/water/methanol/ammonia mixtures, and slurry targets with additional vapor-deposited layers. Mass spectra from the bombardment of these targets will be the subject of future study.

Top priority now rests on the detailed analysis of mass spectra generated through particle impacts into blank targets and thick-films of water ice. The dependence of ejecta on particle mass, particle velocity, target temperature, and accelerating potential will be studied in depth. Focus on water ice spectra will help improve the calibration of the TOF mass spectrometer and yield results that are directly comparable to previous work.[25,11] After spectra generated by impacts into water ice are understood in greater detail, work will shift to pure methanol ice and simple salt water pastes. Target composition is expected to gradually become more complicated until ejecta from impacts into Olivine slurries can be analyzed and explained in detail.

Long term studies with this cryogenic target system will focus on developing answers for key open science questions. These investigations will explore the dependence of impact-produced ejecta yield, angular distribution and kinetic energy on impactor velocity and mass; the characteristics of fast-ejecta components responsive for secondary cratering and the formation of dust exospheres; what is the composition of impact products produced by micrometeoroid bombardment onto ice and icy regolith; and the mapping of ejecta to target and projectile parameters.

Finally, as a result of its flexible design, the chamber can easily be used in conjunction with other instruments for calibration purposes. IMPACT will purchase additional diagnostic instruments, such as an infrared spectrometer, and install these on the ice chamber. Once these instruments are installed, the setup will be capable of simultaneously measuring ion plume and ejecta composition on multiple instruments, allowing for the accurate cross-calibration of detectors. This process can be adapted to suit various types of instruments interested in impacts on icy surfaces, including future science instruments such as SUDA.[16]

V. CONCLUSION

A new cryogenic target has been developed and tested at the Solar System Exploration Research Virtual Institute (SSERVI) IMPACT. This versatile target provides the capability to study hypervelocity micrometeoroid bombardment onto well-controlled icy targets, including vapor-grown ice layers of H_2O, CH_3OH, and NH_3 and pre-frozen mixtures containing nanophase iron. Ice growth under temperatures between 96 K and 150 K can be easily controlled and thickness greater than 150 nm can be measured through an *in situ* interferometry system. Ejecta from dust impacts are analyzed with *in situ* time of flight mass spectroscopy. This target will be used to study the impact phenomena of bombardment into ice and icy regoliths and the formation mechanisms of complex organics found on volatile-rich asteroid surfaces.

ACKNOWLEDGMENTS

This work was supported by the IMPACT of NASA's SSERVI. The authors would like to thank Dan Britt at the University of Central Florida for preparing prototype Olivine samples and John Nibarger at NIST Boulder for the fabrication of sapphire substrates used in vapor-deposited ice trials. The authors would also like to thank the experimental team at IMPACT for the operation of the dust accelerator.

[1]A. T. Basilevsky, A. M. Abdrakhimov, and V. A. Dorofeeva, Sol. Syst. Res. **46**(2), 89 (2012).
[2]L. M. Prockter, Johns Hopkins APL Tech. Dig. **26**, 175 (2005).
[3]M. S. Gudipati and J. Castillo-Rogez, *The Science of Solar System Ices* (Springer, 2012).
[4]S. A. Stern *et al.*, Science **350**(6258), 292 (2015).
[5]M. J. Burchell, M. J. Cole, and P. R. Ratcliff, Icarus **122**, 359 (1996).
[6]M. J. Burchell, I. D. S. Grey, and N. R. G. Shrine, Adv. Space Res. **28**(10), 1521 (2001).
[7]K. Eichhorn and E. Grün, Planet. Space Sci. **41**(6), 429 (1993).
[8]D. Koschny and E. Grün, Icarus **154**, 402 (2001).
[9]R. Timmermann and E. Grün, *Origin and Evolution of Interplanetary Dust* (Springer, 1991), Vol. 375.
[10]F. Postberg, S. Kempf, J. K. Hillier, R. Srama, S. F. Green, N. McBride, and E. Grün, Icarus **193**, 438 (2008).
[11]F. Postberg, S. Kempf, J. Schmidt, N. Brilliantov, A. Beinsen, B. Abel, U. Buck, and R. Srama, Nature **459**, 1098 (2009).
[12]F. Postberg, E. Grün, M. Horányi, S. Kempf, H. Kruger, R. Srama, Z. Sternovsky, and M. Trieloff, Planet. Space Sci. **59**, 1815 (2011).
[13]A. Shu, A. Collette, K. Drake, E. Grün, M. Horányi, S. Kempf, A. Mocker, T. Munsat, P. Northway, R. Srama, Z. Sternovsky, and E. Thomas, Rev. Sci. Instrum. **83**, 075108 (2012).
[14]A. Mocker, S. Bugiel, S. Auer, G. Baust, A. Collette, K. Drake, K. Fiege, E. Grün, F. Heckmann, S. Helfert, J. Killier, S. Kempf, G. Matt, T. Mellert, T. Munsat, K. Otto, F. Postberg, H.-P. Röser, A. Shu, Z. Sternovsky, and R. Srama, Rev. Sci. Instrum. **82**, 095111 (2011).
[15]R. Srama *et al.*, "The Cassini cosmic dust analyzer," in *The Cassini-Huygens Mission* (Springer, 2004), p. 465.
[16]S. Kempf, N. Altobelli, C. Briois, T. Cassidy, E. Grün, M. Horányi, F. Postberg, J. Schmidt, S. Shasharina, R. Srama, and Z. Sternovsky, LPI Contrib. **1774**, 32 (2014).
[17]Z. Martins, M. C. Price, N. Goldman, M. A. Sephton, and M. R. Burchell, Nat. Geosci. **6**, 1045 (2013).
[18]G. Strazzullaand and R. E. Johnson, *Comets in the Post-Halley Era* (Springer, 1991), Vol. 1, pp. 243–275.
[19]C. F. Chyba, P. J. Thomas, L. Brookshaw, and C. Sagan, Science **249**, 366 (1990).
[20]S. A. Bowden, J. Parnell, and M. J. Burchell, Int. J. Astrobiol. **8**(1), 19 (2009).
[21]N. Artemieva and J. Lunine, Icarus **164**, 471 (2003).
[22]M. H. Moore, B. Donn, R. Khanna, and M. F. A'Hearn, Icarus **54**, 388 (1983).
[23]K. Kobayashi, T. Kasamatsu, T. Kaneko, J. Koike, T. Oshima, T. Saito, T. Yamamoto, and H. Yanagawa, Adv. Space Res. **16**, 21 (1995).
[24]M. P. Bernstein, S. A. Sandford, L. J. Allamandola, S. Chang, and M. A. Scharberg, Nature **416**, 401 (2002).
[25]B. L. Henderson and M. S. Gudipati, Astrophys. J. **800**, 66 (2015).
[26]N. J. Sack and R. A. Baragiola, Phys. Rev. B **48**(14), 9973 (1993).
[27]A. Lignell and M. S. Gudipati, J. Phys. Chem. A **119**, 2607 (2015).
[28]A. Mocker, E. Grün, Z. Sternovsky, K. Drake, S. Kempf, K. Hornung, and R. Srama, J. Appl. Phys. **112**, 103301 (2012).